Hindawi Publishing Corporation
International Journal of Antennas and Propagation
Volume 2016, Article ID 4135404, 7 pages
http://dx.doi.org/10.1155/2016/4135404

Research Article

A New Method of Wave Mapping with HF Radar

Lijie Jin, Biyang Wen, and Hao Zhou

Electronic Information School, Wuhan University, Wuhan 430072, China

Correspondence should be addressed to Biyang Wen; bywen@whu.edu.cn

Received 24 March 2016; Revised 2 June 2016; Accepted 4 August 2016

Academic Editor: Björn Lund

Study of wave height inversion with High-Frequency Surface Wave Radars (HFSWRs) has been going on for more than 40 years. Various wave inversion methods have been proposed, and HFSWRs have achieved great success in local wave measurements. However, the method of wave mapping is still under development, especially for the broad-beam HF radars. Existing methods of wave mapping are based on narrow-beam radar with beamforming. This paper introduces a way of wave height inversion, using the ratio of the second-harmonic peak (SHP) to the Bragg peak (RSB). A new wave mapping method is proposed, which can be used in both narrow and broad-beam radars, according to the way of wave inversion based on the RSB. In addition, radar wave measurements at the buoy position are compared with the *in situ* buoy, which show a good agreement. At last, the results of wave mapping on the two-hour timescale are given.

1. Introduction

Extraction of wave height with HFSWRs was started since Barrick [1] deduced the second-order integral equation, relating radar sea echo to the ocean wave spectrum. Various methods of wave height inversion have been proposed, for example, Barrick [2], Wyatt [3], Howell and Walsh [4], Hisaki [5], and so forth. Except for these proposed wave height inversion methods, many research results related to the wave height are also displayed, for example, Gill and Walsh [6], Huang et al. [7], Wyatt [8, 9], and Tian et al. [10]. All of them are proved to be feasible in local wave measurements. However, the method of wave mapping, which can display the wave measurements of a large sea area at the same time, is still under development, especially for the broad-beam HF radars. Obtaining the wave maps is helpful in maritime research activities and offshore operations and so forth. Existing methods of wave mapping are based on narrow-beam radar, both the sky wave radar [11] and the ground wave radar [12]. Wave maps can be achieved every 3–6 h by beamforming and scanning in azimuth, with the Wide Aperture Research Facility (WARF) skywave radar [11]; phased array radar named WEllen RAdar (WERA) is used to map the ocean wave height by digital beam forming (DBF) [12]. Both of the radars have a large aperture, which brings some disadvantages: (1) the radar site requiring a sufficiently narrow and flat coast, which sometimes cannot be satisfied; (2) difficulties in installation and erection; and (3) high costs in operating and maintenance.

A wave height inversion method is introduced, based on the ratios of the SHPs to the Bragg peaks [13]. The Bragg peaks are caused by the waves moving toward or away from radar, with fixed wavenumber $2k_0$ (k_0 being the radar wavenumber). Surface current and wind direction information can be relatively obtained from the Bragg peaks. The second-order echo is observed from either side of the Bragg lines, and important wave information can be derived from this part of the spectrum [2]. Furthermore, some research work has been focused on the second-order echo. Studies by Wyatt [14] and Kingsley et al. [15] suggested that at high sea states this second-order part of the spectrum might change in a way that was not consistent with current theory. Ivonin et al. [16] studied the singularities (including f_B, $\sqrt{2}f_B$, and $2^{3/4}f_B$) in Barrick's formula and showed that SHPs were primarily due to the waves propagating parallel to the radar beam, with the wavenumber k_0. Besides, Zhang et al. [17] observed that the peak at $\sqrt{2}f_B$ was much stronger than the surrounding spectrum and then derived another expression for the SHPs by a boundary perturbation method. Although these theories of SHPs may need further improvement, they are instructive

for potential applications on sea state extraction using these peaks other than the conventional second-order spectral continuum.

In this letter, a new wave mapping method is proposed, according to the way of wave inversion based on the RSB [13]. With the measured antenna patterns, this new method of wave mapping can be used in both narrow and broad-beam HF radars. The azimuth range of wave mapping is about 180 degrees with ground-based radar and 360 degrees with drilling platform. A broad-beam radar with compact cross-loop/monopole antennas is used here, which can receive the sea echo from different azimuths. When currents exist, the first-order spectrum will be broadened. The Bragg peaks from different Directions of Arrivals (DOAs) will be dispersed. Multiple signal classification (MUSIC) [18] is used to estimate DOAs of the Bragg peaks and SHPs. Azimuth of the wave height can be obtained by calculating the Bragg peak's DOA. With the colocated antennas, both the measured and ideal antenna patterns can be used in wave mapping, and measured antenna patterns are used here in MUSIC-based direction finding.

An experiment conducted during 2014 in Fujian Province, China, is introduced in Section 2. Section 3 describes the details of the wave mapping method with broad-beam HF radar. Section 4 shows the results of wave mapping and the comparisons between radar wave measurements and the *in situ* buoy data. Section 5 is dedicated to the summary.

2. Description of Experiment

From September to October in 2014, an experiment was conducted in Fujian Province, China. The radar used is the monostatic HFSWR named Ocean State Measuring and Analyzing Radar type SD (OSMAR-SD) [19] with compact cross-loop/monopole antennas. OSMAR-SD is designed by Wuhan University of China, which is mainly used for sea state monitoring. The Frequency-Modulated Interrupted Continuous-Wave (FMICW) is used with the bandwidth of 60 KHz and the period of 0.27 s; therefore, the range resolution of the radar is 2.5 km.

The radar site, namely, PTAN (25°28.3′N, 119°47.6′E), is shown in Figure 1, with two buoys. Buoy A (25°28.4′N, 119°51.8′E) is about 7.3 km far from PTAN, and the azimuth is 74 degrees (the north is 0 degrees); Buoy B (25°23.8′N, 119°55.8′E) is about 15.3 km, and the azimuth is 116 degrees.

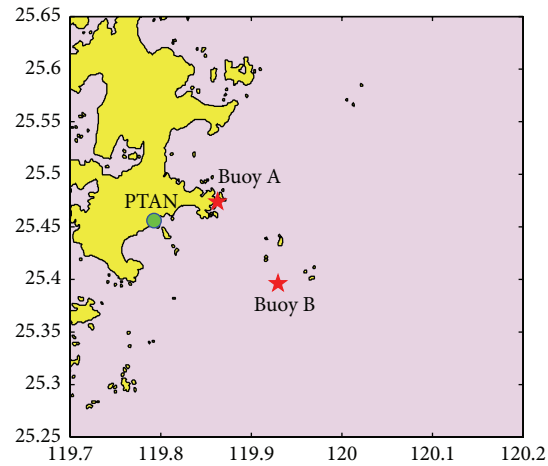

Figure 1: Geographic map of the observation system. PTAN is the radar operating at 13.5 MHz. Buoy A and Buoy B are the two buoys located in the sea area within radar detection range, 7.3 km and 15.3 km far from the radar, respectively.

3. Method

3.1. The Relationship between the RSB and Significant Wave Height. The difference of the second-harmonic peak and the Bragg peak is constant $\Delta f = 0.414 f_B$ (f_B denotes the Bragg frequency) in Doppler domain. The ratio of the second-harmonic peak to the Bragg peak (RSB) r is given by

$$r = 10\log_{10}\left(\frac{P_{\mathrm{SHP}}}{P_B}\right), \quad (1)$$

where P_{SHP}, P_B denote the power of the SHP and the Bragg peak, respectively. After observing the sea echo under different sea states, shown in Figure 2, the different performance of the SHP and the Bragg peak can be summarized as follows:

(1) Under the low sea state, Figure 2(a), $H_s = 1.0$ m (which denotes the significant wave height measured by the buoy), the second-order spectrum is not obvious, almost drowned in the noise, while the first-order spectrum is obvious. The RSB is great, about −21.31 dB.

(2) Figure 2(b) shows that with sea state increasing to the level $H_s = 2.5$ m, the power of the second-order spectrum becomes stronger; however, the power of the first-order spectrum changes only a little, because the Bragg waves are easier to reach saturation. The RSB is about −17.55 dB.

(3) Under the high sea state, Figure 2(c), $H_s = 3.9$ m, the power of the second-order spectrum keeps increasing to a certain degree; meanwhile, the power of the first-order spectrum changes to be smaller. The RSB is about −14.86 dB.

According to the observations of the SHPs and Bragg peaks, it is easy to find that the RSB is closely related to the sea state or significant wave height. That is to say, the RSB changes with the increase of significant wave height. Besides, estimating the DOAs of the Bragg peaks and corresponding SHPs marked in Figures 2(a), 2(b), and 2(c), we can find that the Bragg peak and corresponding SHP come from almost the same direction, shown in Figure 2(d). This conclusion can be certified in [13], which analysed the data from OSMAR-S in Fujian Province during 2013. MUSIC algorithm is adopted in the data analysis of the two experiments. The difference is that measured antenna patterns are used in this paper and ideal antenna patterns in [13]. In the following section, a linear model of the RSB and significant wave height will be

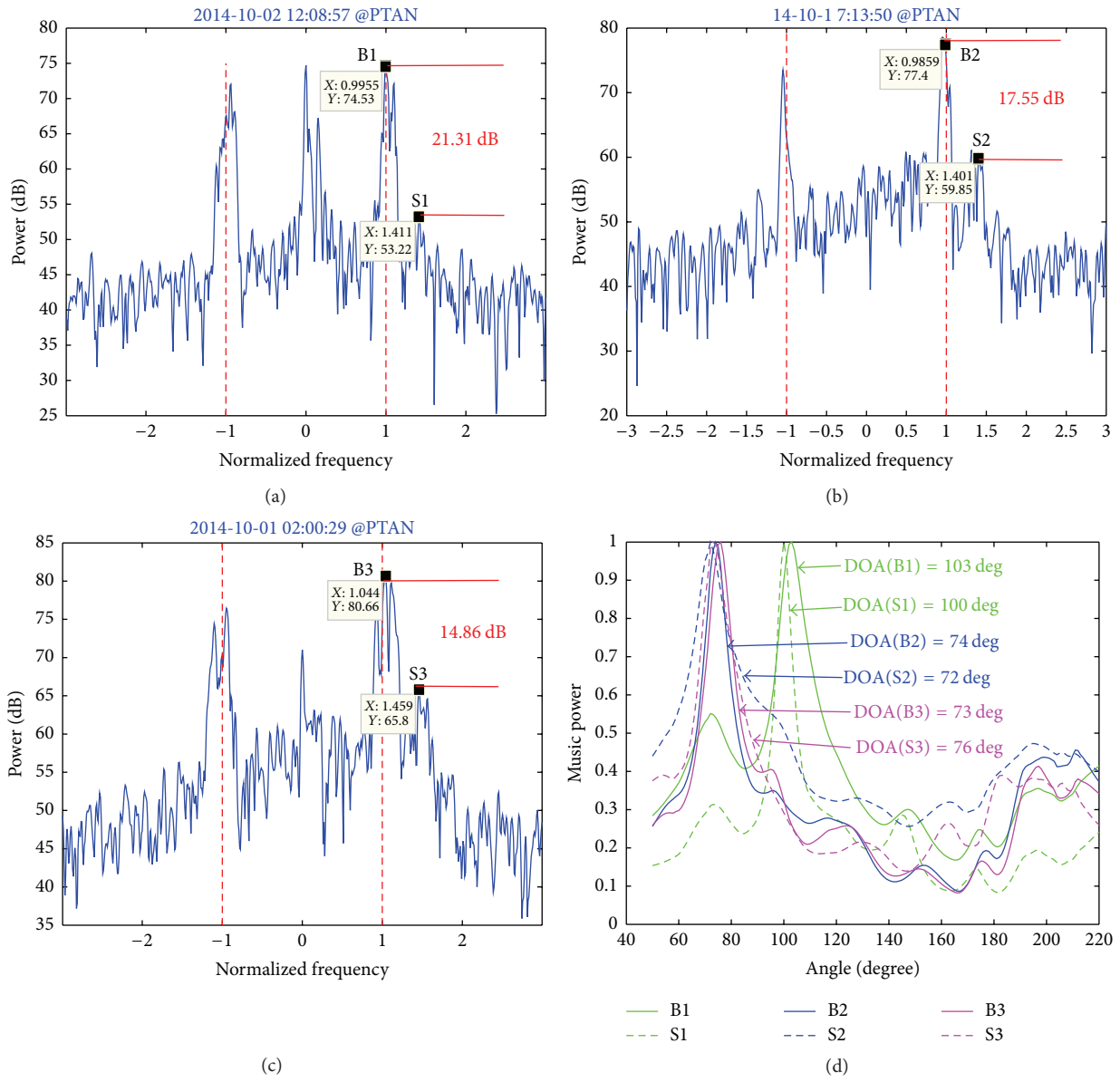

FIGURE 2: Observations of the RSB under different sea state, (a) the low sea state, (b) the normal sea state, (c) the high sea state, and (d) DOAs of the Bragg peaks and corresponding SHPs, estimated with MUSIC.

established, from which radar wave measurements can be extracted.

3.2. The Linear Model of the RSB and Significant Wave Height by Fitting to Wave Buoy Data. Both radar-measured data and wave buoy data are necessary, in order to get the linear model of r and H_s, where r is the RSB and H_s denotes the significant wave height. The content of this section is focused on obtaining the RSBs from radar-measured data.

With broad-beam radar, the first-order spectrum of sea echo becomes broader, including many Bragg peaks from different DOAs. The Doppler spectrum of a fixed range-bin contains many first-order peaks and corresponding SHPs. Consisted of one first-order peak and the corresponding SHP, the couple has two characteristics: the difference of their Doppler shifts being constant $\Delta f = 0.414 f_B$ and coming from almost the same direction. According to the characteristics, the couples can be selected from the Doppler spectrum.

A wave height may correspond to a range of the RSBs, because single RSB has a certain degree of randomness; however, the median of the RSBs is highly related to the buoy wave height. Figure 3 shows the linear model of r and H_s from different directions:

$$\begin{aligned} r &= -23.5 + 3.10 H_s, \\ \text{DOA} &= 70 \text{ deg}, \\ r &= -25.8 + 2.85 H_s, \\ \text{DOA} &= 120 \text{ deg}. \end{aligned} \tag{2}$$

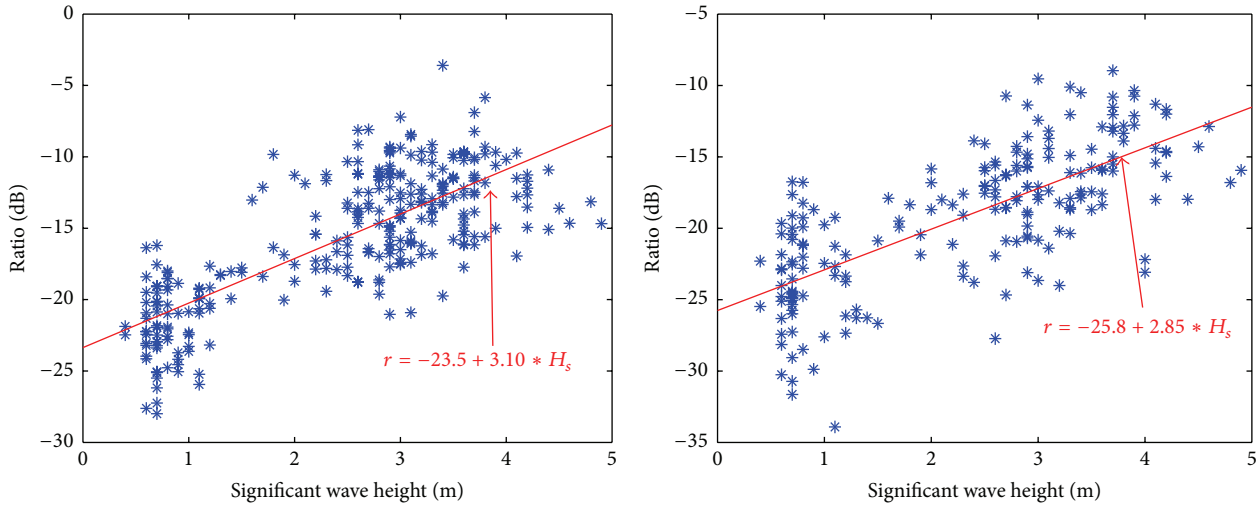

FIGURE 3: Ratios of the SHPs to the Bragg peaks fitted to the wave buoy data: (a) from 70 degrees; (b) from 120 degrees.

The difference among different directions is not great, and the final linear model can be written as

$$r = -A + B \cdot H_s, \tag{3}$$

where A and B are two parameters of the linear model, which may change in different sea areas. In this experiment, the values of A and B are 25 and 3.0, respectively. Based on this linear model, the method of extracting significant wave height is given by

$$H_{\text{radar}} = \frac{(r + A)}{B}, \tag{4}$$

where r denotes the RSB and H_{radar} is the significant wave height measured by radar. Notice that, after some more research work about the Bragg peak and the SHP, we find that the Bragg peak get saturated when sea state increases to the level $H_s \approx 2$ m, and the SHP is $H_s \approx 4$ m, with the radar frequency 13 MHz. When the SHP is unsaturated, the measured H_{radar} is reliable with the linear model. A higher sea state with $H_s > 5$ m requires a lower radar frequency.

3.3. Detail Steps of Wave Mapping. In the above section, the method of wave extraction based on the linear model is introduced. The wave heights measured by radar contain both the range and azimuth information, related to the Bragg peaks.

To map the ocean wave height, the sea area within radar detection range is divided into a series of two-dimensional space grids. The range resolution is set to 2.5 km, according to the range resolution of radar. The azimuth resolution is 10 degrees, considering the bearing error in MUSIC-based direction finding, associated with the signal noise ratio [20]. Besides, the cumulative number of each grid also needs to be considered. The higher azimuth resolution (e.g., 6 or 3 degrees) leads to the less cumulative number, which is not conducive to the robustness of wave extraction.

Considering changes of the sea state, two hours' radar data is used in each wave map. The wave map can be obtained by the following steps.

Step 1. Put all the measured wave heights into the two-dimensional space grids, according to the information of range and azimuth.

Step 2. Calculate the median of wave heights within one certain grid and regard it as the wave height of this grid.

Step 3. If the cumulative number of the grid is less than 3, replace the value with the average wave height of nearby sea area. With few RSBs, the wave height measured from the linear model is not robust, because single RSB has a certain degree of randomness. Therefore, it is necessary to have enough cumulative number for the robust wave measurement.

Step 4. Interpolate the wave map in two-dimensional space with the linear interpolation method [21].

4. Results

In this section, comparisons of the local estimated wave heights versus the buoy data are given. Besides, the results of wave mapping are presented. Two parts of the radar-measured data are selected as examples for wave mapping, 21:00 to 23:00 Sep 27 and 17:30 to 19:30 Oct 9, 2014; the significant wave heights from Buoy B are about 1.8 m and 3.2 m, respectively.

As shown in Figure 4, two-hourly wave measurements from radar are compared with the *in situ* buoys. The radar data used is about 20 days from 10:00 Sep 25 to 8:00 Oct 15, 2014. Both the two local wave measurements show good agreements versus the two buoys, with correlation above 0.8. Except for the similarity, there are some differences between

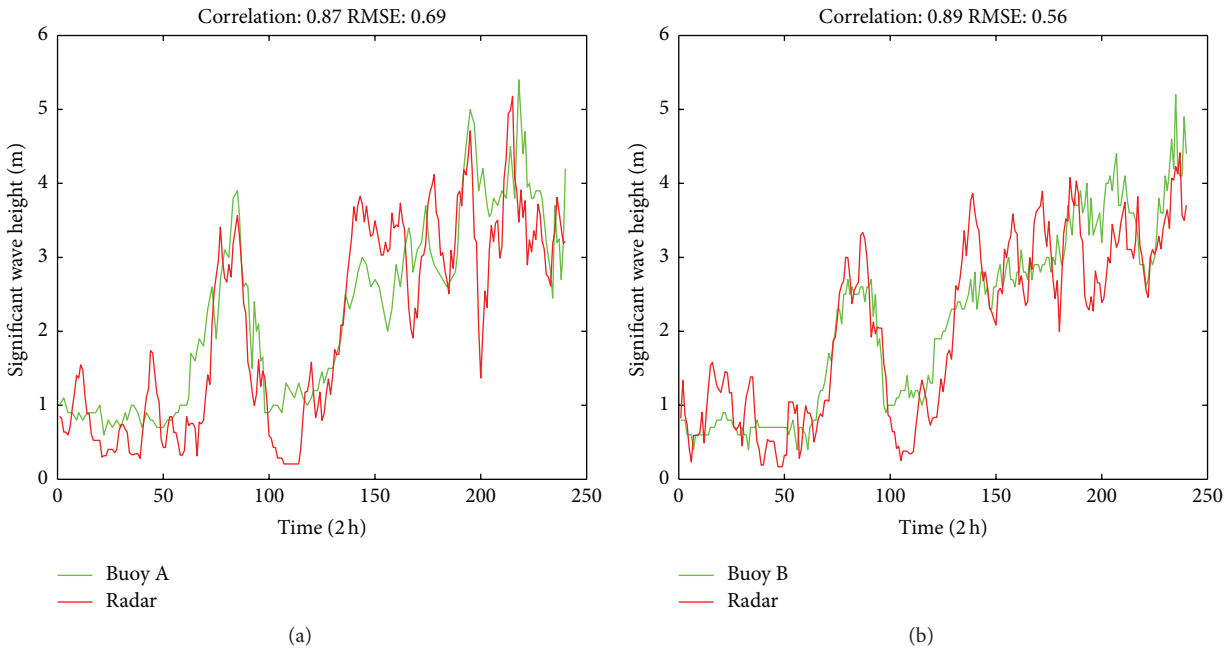

FIGURE 4: The local wave measurements between radar and buoys, time relative to 10:00 Sep 25, 2014. (a) Buoy A; (b) Buoy B.

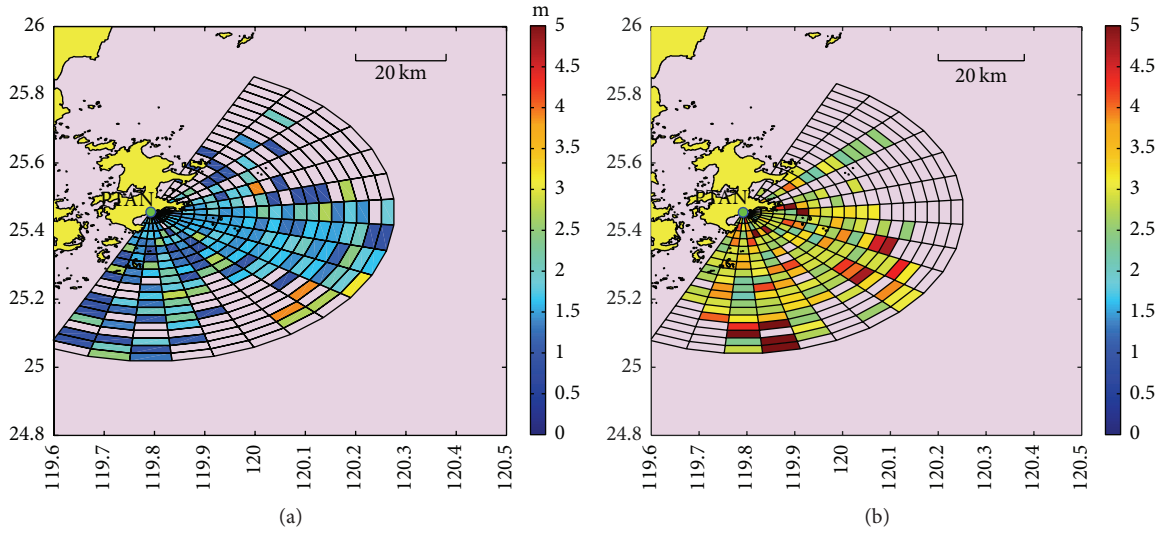

FIGURE 5: The initial wave maps, the sea area is divided into a series of two-dimensional space grids with the range resolution 2.5 km and the azimuth 10 degrees. (a) 21:00 to 23:00 Sep 27, 2014; (b) 17:30 to 19:30 Oct 9, 2014.

Figures 4(a) and 4(b). The comparison from Buoy B performs better than that from Buoy A, with a smaller Root Mean Square Error (RMSE) 0.56 m. A small part of the radar wave measurements is underestimated in Figure 4(a), because the corresponding cumulative number is only one or two. And it may be due to the location of Buoy A, which is much closer to the coast. The two comparisons with the *in situ* buoys indicate that enough cumulative number is important to obtain the robust wave measurements.

Figure 5 shows the initial wave height maps. The azimuth ranges from 20 to 200 degrees with resolution of 10 degrees. The distance ranges from the first to the eighteenth range-bin with resolution of 2.5 km. Some of the two-dimensional space grids are empty without wave heights, mainly distributed in the range from 20 to 70 degrees. A possible reason is the shielding effect of the island, which may attenuate the signal passing through.

Figure 6 displays the wave maps after replacement, which become more gentle compared with the initial wave maps, since most of the overestimated or underestimated wave heights are replaced. Comparing the two wave maps in Figure 6, sea state of Figure 6(a) is lower than that of Figure 6(b). The coverage efficiency of offshore within 20 km is almost the same between the two wave maps. However, it is

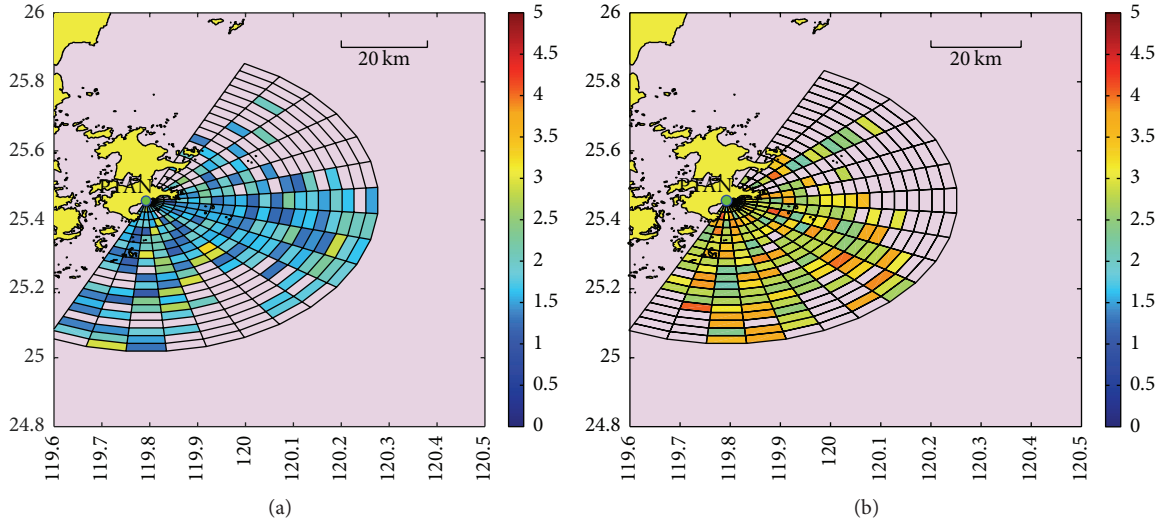

Figure 6: The wave maps after replacement. (a) 21:00 to 23:00 Sep 27, 2014; (b) 17:30 to 19:30 Oct 9, 2014.

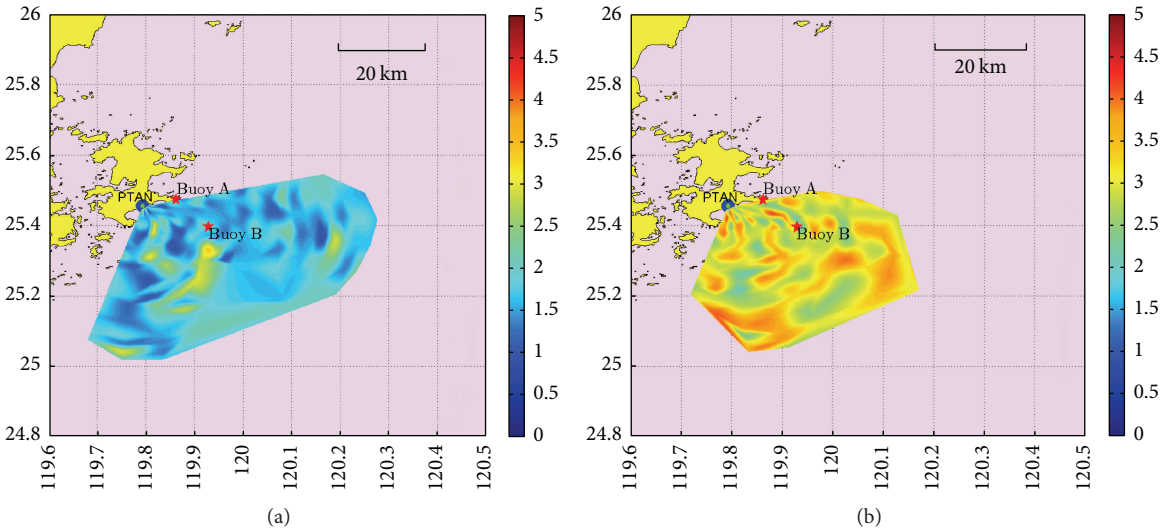

Figure 7: The wave maps after interpolating in two-dimensional space. (a) 21:00 to 23:00 Sep 27, 2014; (b) 17:30 to 19:30 Oct 9, 2014.

different in the further sea areas, which may be due to higher propagation losses in rough seas.

In Figure 7, the final wave maps are obtained after interpolating. The difference between most of the measured wave heights and the *in situ* buoy data is less than 0.5 m, shown in Figure 6. However, there are still a few overestimated or underestimated wave heights in the wave maps after replacement, and the final wave maps may not be so continuous. In addition, the locations of two buoys are marked. Buoy A corresponds to the azimuth of 70 degrees and the third range-bin, while Buoy B is 120 degrees and the sixth range-bin.

5. Summary

In this letter, a method of wave height inversion is introduced, using the linear model of RSB and significant wave height. Based on this method, a new approach to wave mapping is proposed. In this method of wave mapping, MUSIC is used for direction finding, rather than digital beam forming. Therefore, it can be applied in both broad and narrow-beam radars. There is good agreement in comparisons of the local wave measurements from radar and buoys about 20 days, with correlation above 0.8 and RMSE about 0.6 m, which prove the effectiveness of this wave mapping method. Though the final wave maps perform well compared with buoys wave data, there are still some problems to be solved: (1) the linear model of the RSB and significant wave height ($r = -A + B \cdot H_s$) is obtained by fitting to wave buoy data. A new way to obtain the wave data instead of the buoys is necessary, considering the applicability of the wave mapping method. (2) In order to get accurate wave maps, cumulative number of the space lattice should be enough, which is proportional to the timescale of radar-measured data used in each wave

map. Nevertheless, this method still keeps the potentiality to achieve wave maps with both the narrow and broad beam HF radars. Ongoing work will focus on improving the accuracy and robustness of this wave mapping method: for example, (1) conduct more experiments in different places, under different sea states; (2) find a more suitable model instead of the linear model in connecting RSB with the significant wave height; and (3) make a comparison between the measured and ideal antenna patterns in wave mapping.

Competing Interests

The authors declare that they have no competing interests.

Acknowledgments

The authors would like to thank the Fujian Marine Bureau for the buoys data provided.

References

[1] D. Barrick, "Remote sensing of sea state by radar," in *Proceedings of the IEEE International Conference on Engineering in the Ocean Environment (Ocean '72)*, pp. 186–192, Newport, RI, USA, September 1972.

[2] D. E. Barrick, "Extraction of wave parameters from measured hf radar sea-echo doppler spectra," *Radio Science*, vol. 12, no. 3, pp. 415–424, 1977.

[3] L. R. Wyatt, "A relaxation method for integral inversion applied to HF radar measurement of the ocean wave directional spectrum," *International Journal of Remote Sensing*, vol. 11, no. 8, pp. 1481–1494, 1990.

[4] R. Howell and J. Walsh, "Measurement of ocean wave spectra using narrow-beam HF radar," *IEEE Journal of Oceanic Engineering*, vol. 18, no. 3, pp. 296–305, 1993.

[5] Y. Hisaki, "Ocean wave directional spectra estimation from an HF ocean radar with a single antenna array: methodology," *Journal of Atmospheric and Oceanic Technology*, vol. 23, no. 2, pp. 268–286, 2006.

[6] E. W. Gill and J. Walsh, "Extraction of ocean wave parameters from HF backscatter received by a four-element array: analysis and application," *IEEE Journal of Oceanic Engineering*, vol. 17, no. 4, pp. 376–386, 1992.

[7] W. Huang, S.-C. Wu, E. Gill, B.-Y. Wen, and J.-C. Hou, "HF radar wave and wind measurement over the Eastern China Sea," *IEEE Transactions on Geoscience and Remote Sensing*, vol. 40, no. 9, pp. 1950–1955, 2002.

[8] L. R. Wyatt and J. J. Green, "Measuring high and low waves with HF radar," in *Proceedings of the IEEE Bremen: Balancing Technology with Future Needs (OCEANS '09)*, pp. 1–5, Bremen, Germany, May 2009.

[9] L. R. Wyatt, "Significant waveheight measurement with h.f. radar," *International Journal of Remote Sensing*, vol. 9, no. 6, pp. 1087–1095, 1988.

[10] Y.-W. Tian, B.-Y. Wen, and H. Zhou, "Measurement of high and low waves using dual-frequency broad-beam HF radar," *IEEE Geoscience and Remote Sensing Letters*, vol. 11, no. 9, pp. 1599–1603, 2014.

[11] J. W. Maresca Jr., T. M. Georges, C. T. Carlson, and J. P. Riley, "Two tests of real-time ocean wave-height mapping with hf skywave radar," *IEEE Journal of Oceanic Engineering*, vol. 11, no. 2, pp. 180–186, 1986.

[12] L. R. Wyatt, "Wave mapping with HF radar," in *Proceedings of the IEEE/OES 10th Working Conference on Current, Waves and Turbulence Measurement (CWTM '11)*, pp. 25–30, Monterey, Calif, USA, March 2011.

[13] H. Zhou and B.-Y. Wen, "Observations of the second-harmonic peaks from the sea surface with high-frequency radars," *IEEE Geoscience and Remote Sensing Letters*, vol. 11, no. 10, pp. 1682–1686, 2014.

[14] L. Wyatt, "The measurement of the ocean wave directional spectrum from hf radar doppler spectra," *Radio Science*, vol. 21, no. 3, pp. 473–485, 1986.

[15] S. P. Kingsley, A. Matoses, and L. R. Wyatt, "Analysis of second order HF radar sea spectra recorded in storm conditions," in *Proceedings of the IEEE OCEANS '98 Conference*, vol. 1, pp. 459–462, IEEE, Nice, France, 1998.

[16] D. V. Ivonin, V. I. Shrira, and P. Broche, "On the singular nature of the second-order peaks in HF radar sea echo," *IEEE Journal of Oceanic Engineering*, vol. 31, no. 4, pp. 751–767, 2006.

[17] S.-S. Zhang, B.-Y. Wen, and H. Zhou, "Analysis of the higher order Bragg scatter in HF radar," *Journal of Electromagnetic Waves and Applications*, vol. 27, no. 4, pp. 507–517, 2013.

[18] T. De Paolo, T. Cook, and E. Terrill, "Properties of HF RADAR compact antenna arrays and their effect on the MUSIC algorithm," in *Proceedings of the Oceans*, pp. 1–10, IEEE, Vancouver, Canada, October 2007.

[19] Y. Tian, B. Wen, J. Tan, K. Li, Z. Yan, and J. Yang, "A new fully-digital HF radar system for oceanographical remote sensing," *IEICE Electronics Express*, vol. 10, no. 14, 2013.

[20] T. Paolo, T. Cook, and E. Terrill, "Properties of HF radar compact antenna arrays and their effect on the MUSIC algorithm," in *Proceedings of the OCEANS 2007*, pp. 1–10, IEEE, Vancouver, Canada, 2007.

[21] D. Watson, *Contouring: A Guide to the Analysis and Display of Spatial Data*, Pergamon Press, Oxford, UK, 1992.